Research Square

Preprints are preliminary reports that have not undergone peer review.
They should not be considered conclusive, used to inform clinical practice,
or referenced by the media as validated information.

Network Pharmacology, Molecular Docking, and Molecular Dynamics Simulation Analysis Reveal Insights into the Molecular Mechanism of Schizandrin A in Treating Age-related Hearing Loss

Liangliang Wang

wlljy80@163.com

Macau University of Science and Technology

Jing Sun

Nanxishan Hospital, Guangxi Zhuang Autonomous Region

Lili Yu

Macau University of Science and Technology

Qianghe Liu

The First Affiliated Hospital of Guilin Medical University

Fangxian Liu

The First Affiliated Hospital of Guilin Medical University

Article

Keywords: Age-related hearing loss, Schisandrin A, molecular docking, molecular dynamics, network pharmacology

Posted Date: November 17th, 2026

DOI: https://doi.org/10.21203/rs.3.rs-11520077/v1

License: This work is licensed under a Creative Commons Attribution 4.0 International License.
Read Full License

Additional Declarations: No competing interests reported.

Abstract

Age-related hearing loss (ARHL) is a bilateral, symmetrical, and progressive sensorineural disorder associated with aging and represents a major public health challenge in aging societies. Schisandrin A (SchA), a biphenylocyclooctene-type lignan monomer isolated from the dried fruits of Schisandra chinensis, exhibits antioxidant and anti-inflammatory effects, regulates mitochondrial autophagy, and inhibits apoptosis. This study aimed to investigate the potential molecular mechanisms underlying the therapeutic effects of Sch A against ARHL using network pharmacology, molecular docking, and molecular dynamics (MD) simulations. Network pharmacology identified 137 potential targets. Gene ontology (GO) enrichment analysis revealed that these genes mediate cellular signaling responses, ion balance, and physiological homeostasis through kinase cascade signaling, ion channel regulation, and synaptic signal transmission. Kyoto encyclopedia of genes and genomes pathway enrichment analysis identified calcium and cAMP signaling pathways, neuroactive ligand signaling, and neuroactive ligand-receptor interactions as major enriched pathways. Molecular docking and MD simulations were used to screen binding affinities. The binding energies for SRC, STAT3, EGFR, HSP90AA1, HIF1A, and PTGS2 were all lower than − 5.0 kcal/mol, indicating high binding affinity and stable binding modes. Among these, PTGS2 exhibited the lowest binding energy. MD simulation revealed that the PTGS-deoxyschizandrin complex had an overall average root mean square deviation (RMSD) of 0.18 nm, a protein backbone and ligand RMSD of 0.22 and 0.09 nm, respectively. The mean radius of gyration and solvent-accessible surface area were 3.16 and 443.21 nm, respectively, suggesting that the complex did not undergo significant expansion or contraction. The average root mean square fluctuation values for A and B chains of PTGS were 0.12 and 0.13 nm, respectively, indicating low overall flexibility and a relatively stable conformation. The complex formed strong hydrogen bonds, potentially exerting a neuroprotective effect. This study demonstrated the potential molecular mechanisms underlying the effects of Sch A against ARHL and provides a theoretical basis for its application and further drug development.

1. Introduction

Age-related hearing loss (ARHL) is a bilateral, symmetrical, and progressive sensorineural disorder associated with aging and primarily manifests as high-frequency hearing loss[1]. Its prevalence is increasing annually, making it a major public health challenge worldwide[2–3]. The pathological changes associated with ARHL primarily include degeneration of cochlear hair cells, the stria vascularis, spiral ganglion neurons, afferent and efferent auditory pathways, and the auditory cortex[4–5]. Emerging evidence also implicates dysregulation of the cochlear inflammatory microenvironment in the onset and progression of ARHL. With advancing age, impaired immune regulation, diminished antioxidant defenses, disruption of the blood-cochlear barrier, and persistent pro-inflammatory signaling can compromise cochlear homeostasis, leading to pathological remodeling and damage to hair cells, synapses, and auditory nerves[6–7]. Systemic chronic low-grade inflammation, metabolic disorders, and

vascular dysfunction may further exacerbate cochlear inflammation[8–9], highlighting potential avenues for developing new therapeutic strategies for ARHL.

Schisandrin A (SchA) is a biphenylocyclooctene-type lignan monomer isolated from the dried fruits of Schisandra chinensis. It exhibits good fat solubility and is one of the core active components of Schisandra chinensis[10]. Basic research over the past five years has confirmed that SchA exhibits antioxidant and anti-inflammatory effects, modulates mitochondrial autophagy, and inhibits apoptosis, indicating potential pharmacological effects in neurodegenerative diseases, liver injury, tumors, and inflammatory diseases[11–12]. In neuroprotection, SchA can target multiple inflammatory and oxidative stress pathways and exerts protective effects against neuronal damage in Alzheimer's and Parkinson's disease models[13]. However, studies on SchA intervention in ARHL remain limited, and its protective effects on auditory neurons, including cochlear spiral ganglion cells and cochlear hair cells, as well as its molecular targets, remain unclear.

Network pharmacology utilizes static algorithms to collect large datasets from extensive databases, facilitating exploration of interactions among drug components, targets, and disease mechanisms. This approach is widely used to predict the mechanisms of active ingredients in traditional Chinese medicine[14]. Molecular docking is a virtual screening technique that predicts the binding sites and measures interaction strength between a drug and its target, revealing molecular interactions and predicting binding modes and affinities. MD simulations monitor molecular movements and interactions over time, offering insights into molecular conformations and kinetics to assess molecular docking reliability[15]. Therefore, this study examined the mechanism of action of Schisandrin A in treating age-related hearing loss, offering theoretical support and guidance for future research. This provides valuable insights into the molecular mechanisms by which Schisandrin A mitigates age-related hearing loss and expedites the drug discovery process. However, additional cellular and animal experiments are required for validation and analysis. Figure 1 depicts our specific workflow.

2. Materials and Methods

2.1 Prediction of Drug Component Targets

The SMILES notation for Sch A was retrieved from PubChem (https://pubchem.ncbi.nlm.nih.gov/). Target information was obtained from Swiss Target Prediction (http://swisstargetprediction.ch/) and Super-PRED (https://prediction.charite.de/index.php). Target protein annotations were verified using UniProt using "Reviewed" and "Human" criteria.

2.2 Identification of Disease-related Targets and Prediction of Potential Therapeutic Targets

Disease-related targets were retrieved from GeneCards (https://www.genecards.org/) and OMIM (https://omim.org/), and subsequently combined and deduplicated. Potential therapeutic targets were

identified by intersecting the drug targets with the disease-related targets. Venn diagrams were generated using the “venndiagrams” Package.

2.3 Construction of Drug-Component-Disease Target Network

The intersection targets associated with the drug, its individual components, and the diseases were imported into the Cytoscape 3.7.2 visualization tool to construct a drug-component-disease-target network.

2.4 Construction of Protein-Protein Interaction Network

To investigate the protein-protein interactions potentially underlying the disease-modifying effects of SchA, the genes corresponding to the drug-disease intersection were uploaded to STRING (https://string-db.org/) to construct a protein-protein interaction (PPI) network, with the species set to “Homo sapiens.” The results were saved in TSV format and imported into Cytoscape 3.7.2. Topological analysis was performed using the CytoNCA plugin. Core targets were identified based on median betweenness centrality (BC), closeness centrality (CC), and degree centrality (DC) scores. Node size and color were mapped to degree values to visualize the core protein interaction network diagram.

2.5 GO Enrichment Analysis

GO enrichment analysis of the intersecting target genes was performed using R packages “clusterProfiler,” “org.Hs.eg.db,” “enrichplot,” and “ggplot2.” The screening threshold was set at $P < 0.05$. The top 10 enriched terms in each GO functional category (BP, CC, and MF) were selected. The results were visualized using MicroBioinformatics.

2.6 KEGG Pathway Analysis

KEGG pathway enrichment analysis was performed on the intersecting targets using the `library(“pathview”)package and the enrichKEGG function from the R software clusterProfiler package[16–18]. The selection criterion was set at $P < 0.05$. The top 10 pathways were selected based on relevant literature and plotted using a bubble plot.

2.7 Molecular Docking

The chemical structure of Schisandrin A, used as the ligand, was retrieved from the PubChem database (https://pubchem.ncbi.nlm.nih.gov/). Core target proteins were selected as receptors, and the UniProt database (https://www.uniprot.org/) was used to identify the corresponding target receptor protein ID labeled “Human.” After copying the ID, the structural file for the receptor protein was downloaded from the Protein Data Bank (http://www.rcsb.org/pdb). Molecular docking of the protein and small molecule was performed using AutoDock Vina software (version 1.1.2).

2.8 MD Simulation

GROMACS 2022.2[19] was utilized for MD simulation of the protein-ligand complex. The receptor protein topology was generated using pdb2gmx with the Amber99SB-ILDN force field[20]; ligand topology and parameters were constructed using sobtop_1.0 (dev3.1) based on the GAFF2 force field[21], with RESP charge assignment. The system was solvated in a cubic box using the TIP3P water model, with a minimum protein-box edge distance of 1.0 nm; 0.15 M NaCl was introduced via gmx genion. Long-range electrostatics utilized PME, with van der Waals and short-range electrostatic cutoffs of 1.2 nm; bonds were constrained using LINCS, and the integration time step was set to 2 fs. Energy minimization was performed using the steepest descent algorithm, followed by Conjugate Gradient; 1 ns NVT and 1 ns NPT equilibration were performed with positional constraints. The system was subsequently maintained at 300 K and 1 bar using V-rescale (τt = 1 ps) and Parrinello-Rahman (τp = 1 ps). After equilibration, position-unconstrained MD simulations were conducted. The root mean square deviation

(RMSD), root mean square fluctuation (RMSF), radius of gyration (Rg), solvent-accessible surface area (SASA), and protein-ligand hydrogen bonds were calculated. A free energy landscape (FEL) was constructed using PCA and gmx sham.

3. Results

3.1 Collection of Drug Targets

Sch A was searched in PubChem, and its potential target information was obtained from SwissTargetPrediction and Super-PRED. Targets were corrected in UniProt, consolidated, and deduplicated based on “Reviewed” and “Human” criteria, yielding 217 targets for Sch A.

3.2 Collection of Targets for Age-related Hearing Loss and Prediction of Potential Therapeutic Targets for Drugs

GeneCards and OMIM were searched using “Presbycusis” and “age-related hearing loss.” After aggregation and deduplication, 4,842 presbycusis-related targets were identified. Intersection with Sch A targets yielded 137 target molecules for ARHL treatment. Venn diagrams were plotted utilizing “VennDiagrams.”(Fig. 2A)

3.3 Construction of Drug-Compound-Disease Target Network

Cytoscape 3.7.2 was utilized to construct a “Schisandrin A-Compound-Disease Target” network linking Sch A with 137 ARHL-associated targets. The network comprised 139 nodes and 274 edges(Fig. 2B). Pink, green, and purple represented potential targets, drugs, and diseases, respectively.

3.4 PPI Network Construction and Core Target Screening

The 137 potential therapeutic targets were imported into STRING. The species was set to “Homo sapiens,” “minimum required interaction score” was set to 0.4, free-floating targets were hidden, and the remaining parameters were set to default, constructing a PPI network with 132 nodes and 943 edges. Results were imported into Cytoscape 3.7.2 for topological analysis using the CytoNCA plugin. Two rounds of screening based on median BC, CC, and DC scores identified 15 core targets. The top six targets with the highest degree were identified as potential core targets: SRC, STAT3, EGFR, HSP90AA1, HIF1A, and PTGS2(Figs. 3A-B). These targets occupy central positions in the network analysis and may serve as core targets for ARHL treatment with SchA.

3.5 Results of GO Enrichment Analysis

GO enrichment analysis was performed on 137 prospective therapeutic targets using clusterProfiler, org.Hs.eg.db, enrichplot, and ggplot2. The screening threshold was $P < 0.05$. In total, 1,756 biological processes, 99 cell components, and 187 molecular functionalities were enriched. Bar charts were generated for the top 10 enriched functions. At the biological process level, genes were predominantly enriched in response to external stimuli, second messenger-mediated signal transduction, calcium ion transport and intracellular concentration regulation, positive regulation of the mitogen-activated protein kinase (MAPK) cascade, and blood pressure regulation. This indicates their involvement in ion homeostasis, signal transduction, and cardiovascular function. At the cellular component level, enrichment was concentrated in membrane rafts, membrane microdomains, glutamatergic synapses, interneuronal synapses, and synaptic membranes, highlighting roles in membrane signal reception and neural signal transmission. At the molecular function level, genes were characterized by kinase catalytic functions, including transmembrane receptor protein kinase activity, protein serine/threonine kinase activity, protein tyrosine kinase activity, neurotransmitter receptor activity, ligand-gated ion channel activity, and p53 binding(Fig. 4A). These genes systematically facilitate cellular signal responses, ion balance, and physiological homeostasis via kinase cascade signaling, ion channel modulation, and synaptic signal transmission.

3.6 Results of KEGG Pathway Enrichment Analysis

KEGG enrichment analysis was performed on 137 potential targets, utilizing the pathview package and enrichKEGG from clusterProfiler. With $P < 0.05$, 159 signaling pathways were significantly enriched. Based on relevant literature, the top 10 pathways were selected and plotted as a bubble chart. The target genes were primarily enriched in the calcium signaling pathway and in pathways related to central carbon metabolism in cancer, the HIF-1 signaling pathway, fluid shear stress and atherosclerosis, the cAMP signaling pathway, neuroactive ligand signaling, neuroactive ligand-receptor interactions, MAPK signaling pathway, Rap1 signaling pathway, and prostate cancer-related pathways(Fig. 4B).

3.7 Molecular Docking

Sch A was selected as the ligand. The SDF structure was retrieved from PubChem and converted to a 3D conformation in PDB format with the lowest free energy using Open Babel 2.3.2 and Chembio3D. Six

core PPI targets (SRC, STAT3, EGFR, HSP90AA1, HIF1A, and PTGS2) were selected as receptor proteins. The corresponding “Human” receptor protein IDs were retrieved from UniProt, and receptor proteins were retrieved from the Protein Data Bank. Receptor proteins were imported into PyMOL 2.3.4 for dehydration, ligand removal, hydrogenation, and nonpolar hydrogen addition and subsequently converted to a suitable format. Furthermore, hydrogenation was performed utilizing AutoDockTools. The Grid function in AutoDockTools 1.5.6 identified active pockets. Molecular docking was performed utilizing AutoDock Vina 1.1.2(Figs. 5A-F). All reported docking scores for all five proteins with all five ligands were below −5, indicating stable docking results(Table 1)

Table 1

Receptor	Uniport-ID	PDB-ID	Ligand	Binding energy
EGFR	P00533	5ug8	Deoxyschizandrin	-5.8
HIF1A	Q16665	4h6j	Deoxyschizandrin	-5.8
HSP90AA1	P07900	1uyl	Deoxyschizandrin	-5.7
PTGS	P35354	5f19	Deoxyschizandrin	-7.3
SRC	P12931	1o43	Deoxyschizandrin	-5.8
STAT3	P40763	6njs	Deoxyschizandrin	-5.5

3.8 MD Simulation

PTGS2, which exhibited the lowest binding energy, was selected for RMSD and RMSF analysis. RMSD results revealed that the PTGS-deoxyschizandrin complex reached equilibrium and maintained overall structural stability. The average overall RMSD was 0.18 nm, with an RMSD of 0.22 nm for the protein backbone and 0.09 nm for the ligand(Fig. 6A), signifying that the ligand’s position within the binding pocket is highly stable.

Further analysis revealed that the mean Rg and mean SASA of PTGS-deoxyschizandrin complex were 3.16 nm and 443.21 nm, respectively (Figs. 6B-C). These results suggest that the complex did not undergo significant expansion or contraction.

Hydrogen bonds are essential in ligand-protein binding. During stimulation, the number of hydrogen bonds between the PTGS-deoxyschizandrin small molecule and the target protein ranged from 0 to 3(Figs. 6D); in most cases, the complex contained approximately 2 hydrogen bonds, signifying strong hydrogen-bond interactions.

RMSF was used to assess the flexibility of amino acid residues. The average RMSF values for chains A and B of PTGS were 0.12 and 0.13 nm, respectively, indicating relatively low overall flexibility and stable conformation(Figs. 6E).

FEL is illustrated in Fig. 6F. Red regions represent higher free energy, whereas blue regions represent lower free energy. The PTGS-deoxyschizandrin complex system exhibited a prominent low-energy conformational basin, suggesting that the simulation primarily converges to a dominant stable conformation.

Overall, the PTGS-deoxyschizandrin complex system exhibits stable binding and strong hydrogen bonding. Therefore, the small molecule binds well to the target protein.

4. Discussion

ARHL is a common otolaryngological condition whose prevalence increases annually with aging, especially among adults aged ≥ 55. Approximately 40% of individuals aged ≥ 65 experience hearing impairment, making ARHL a major global health concern[22–23]. Beyond its effects on hearing and social burdens, patients with ARHL are more prone to social isolation, depression, and cognitive decline. Additionally, ARHL imposes a significant economic burden on patients and society[24–25].

The pathophysiological mechanisms of ARHL are complex, primarily involving degeneration of cochlear neurons and the auditory cortex, oxidative stress, excessive autophagy, dysregulated cellular signaling, and metabolic alterations[26–27]. Increasing evidence indicates that chronic low-grade inflammation and immune responses play key roles in ARHL onset and progression[28]. Using reverse transcription polymerase chain reaction array analysis, Uraguchi et al.[29] found that in the cochleae of 12-month-old ARHL mice, 40 immune-related genes (47.6%) were differentially regulated, involving cytokine-cytokine receptor interactions, chemokine signaling, TNF signaling, and Toll-like receptor signaling. The NF-κB subunit Nfkb1 was significantly upregulated in aged cochleae, indicating interaction with regulatory regions of genes, including TNF and PTGS2. Gu et al.[30]further demonstrated through bioinformatics analysis that inflammation-related differentially expressed genes were primarily enriched in MAPK, PI3K-Akt, Hippo, and JAK-STAT pathways, supporting a potential role for inflammation in ARHL.

SchA is the primary biphenylocyclooctene-type lignan active compound isolated from the dried fruits of the traditional Chinese medicinal plant Schisandra chinensis[31]. Previous studies have demonstrated that SchA promotes neuronal autophagy, attenuates inflammatory responses and oxidative stress, enhances neurotrophic activity, and exerts neuroprotection on neurons[32]. Another study demonstrated that SchA exerts neuroprotective effects by reducing neuronal atrophy. This study found that SchA significantly increased synaptophysin expression and reduced α-synuclein levels in brain tissue[33]. Accordingly, SchA has garnered increasing attention in research on the alleviation of ARHL.

Here, we integrated network pharmacology, molecular docking, and MD simulations to investigate the active components of SchA and its mechanisms of action in treating ARHL. Based on the current network pharmacology analysis results, we have successfully identified and clarified the potential pharmacological activities and mechanisms of SchA and revealed all core targets of SchA for ARHL. The top six targets, ranked by their degree values, were identified as potential core targets: SRC, STAT3,

EGFR, HSP90AA1, HIF1A, and PTGS2. Moreover, SRC is a non-receptor tyrosine kinase and a member of the Src family of kinases essential in regulating neuronal survival and death[34]. In the auditory system, the SRC-PTK signaling cascade is closely associated with noise-induced hearing loss. Harris et al. reported that SRC inhibitors effectively protect the cochlea from hearing damage caused by a 4-h exposure to 106 dB noise at 4 kHz, signifying that the SRC kinase is a key signaling molecule in noise-induced cochlear damage[35]. STAT3 is a central transcription factor in the JAK-STAT signaling pathway and plays an essential role in cochlear development and the response to injury. Studies have demonstrated that STAT3 expression in the Corti organ of embryonic mice is primarily localized to outer hair cells, where it may participate in regulating their differentiation and survival[36]. The epidermal growth factor receptor (EGFR) contributes to the regeneration of auditory hair cells and to auditory protection. A research team at Stanford University identified a core signaling pathway comprising F2RL1, HBEGF, EGFR, and ERK by studying changes in gene expression in chicken supporting cells following the death of auditory hair cells[37]. In mammals, EGFR signaling is similarly involved in noise-induced hearing loss. Recent in vivo transcriptomic screening revealed that EGFR inhibitors, including afatinib and zorifertinib, can effectively protect mice from noise-induced hearing loss, and conditional EGFR knockout exerts a similar otoprotective effect[38]. HSP90AA1 is an ATP-dependent molecular chaperone that plays a central role in protein folding, stabilization, and degradation. Studies have demonstrated that Hsp90aa1-knockout mice exhibited improved axonal regeneration and reduced macrophage infiltration as early as 2 weeks after nerve transection, signifying that HSP90AA1 may influence nerve regeneration by regulating the inflammatory microenvironment [39]. HIF1A is a central transcription factor in the cellular response to hypoxia and plays a complex role in the cochlea's pathophysiology. A recent study by Liu et al. revealed that HIF1A accumulates in the basilar membrane of the intact cochlea, and this accumulation is rapidly eliminated during in vitro culture[40]. Furthermore, HIF1A plays a positive role in cochlear protection. Studies have demonstrated that upregulating HIF-1α with cobalt chloride (CoCl2) significantly prevents hearing loss in mice exposed to noise; HIF-1α is upregulated in cochlear tissue, and hearing loss is largely prevented[41]. PTGS2, also known as cyclooxygenase-2 (COX-2), is the rate-limiting enzyme that converts arachidonic acid into prostaglandin H2 (PGH2), which is further converted by downstream synthases into prostaglandins, including PGE2. PTGS2 is scarcely expressed in normal tissues but can be rapidly induced by inflammatory stimuli, growth factors, and cytokines. The PTGS2/PGE2 pathway has been implicated in the interplay between ferroptosis and neuroinflammation, and its central role in neuroinflammation has been widely recognized[42–43]. Zhuang et al. reported that PTGS2 inhibition reversed the regulatory effects of miR-125b suppression on neurite outgrowth, apoptosis, and pro-inflammatory cytokines. FOXQ1 and PTGS2 inhibition can reverse these effects, implying that PTGS2 plays a fine-tuned regulatory role in the process of neural repair[44]. Direct evidence has been obtained regarding PTGS2 expression in the cochlea and its significance in ARHL. Studies have demonstrated that PTGS2 is widely expressed in the cochlea of 12-month-old ARHL mice in structures such as the lateral wall (vascular stria and spiral ligament) and is closely associated with the NF-κB regulatory network. Min et al. reported that active components of Schisandra chinensis can form a stable complex with PTGS2[45]. Our study found that, based on GO functional enrichment analysis, these

genes systematically mediate cellular signaling responses, ion balance, and the maintenance of physiological homeostasis via kinase cascade signaling, ion channel regulation, and synaptic signal transmission. Therefore, modulating these key targets can, to a certain extent, influence the activity of cochlear neurons. KEGG pathway enrichment analysis revealed that these genes are mainly enriched in the calcium signaling pathway and also span central carbon metabolism in cancer, HIF-1 signaling pathway, fluid shear stress and atherosclerosis, cAMP signaling pathway, neuroactive ligand signaling, neuroactive ligand-receptor interactions, MAPK signaling pathway, Rap1 signaling pathway, and pathways associated with prostate cancer. Molecular docking revealed that the docking scores for all five proteins with the five components were < -5, signifying stable binding; among them, PTGS2 exhibited the lowest binding energy. MD simulation results of this study suggest that the PTGS-deoxyschizandrin complex is stable and exhibits strong hydrogen bonding; the small molecule binds well to the target protein. This indicates that deoxyschizandrin may serve as an effective PTGS2 inhibitor, potentially establishing it as a promising therapeutic target for age-related hearing loss by alleviating the condition through the pathological processes mentioned above.

This study has several limitations. First, these results were obtained from the literature and databases; due to the incomplete coverage of public databases, potential predictive biases exist, and therefore, their reliability and accuracy depend on data quality. Second, the lack of evidence to substantiate our conclusions highlights the need for in vitro and in vivo experiments to confirm these findings. Third, experimental validation is essential for further confirming the affinity of Schisandrin A for key targets. Until computational predictions are experimentally validated, our conclusions remain preliminary. Consequently, future research should focus on conducting comprehensive in vitro and in vivo studies on Schisandrin A's effects on age-related hearing loss, and high-quality clinical trials to fully confirm its efficacy and safety. Concurrently, we will expand the scope of analysis and comprehensively apply strategies, including multi-omics, to more thoroughly clarify the mechanism of action of Schisandrin A.

5. Conclusions

This study integrated network pharmacology, molecular docking, and MD simulations to investigate the potential molecular mechanisms underlying the effects of Schisandrin A on ARHL. Network analysis highlighted the multi-targeted nature of Schisandrin A, which concurrently influences multiple pathways associated with the progression of ARHL. Schisandrin A exerts its effects by acting on targets, including SRC, STAT3, EGFR, HSP90AA1, HIF1A, and PTGS2. Specifically, the identification of the PTGS2 gene as a potential therapeutic target offers a potential avenue for ARHL prevention and intervention, with the prospect of improving treatment outcomes. Despite these advances, it is worth noting that this study has limitations, and further cellular and animal experiments are required to confirm and expand upon our findings. Adverse reactions associated with traditional PTGS2 inhibitors have limited their clinical application. Traditional Chinese medicine provides unique advantages, and Schisandrin A, as a natural inhibitor, holds promising prospects for development. This study establishes a robust scientific framework for investigating the therapeutic potential of Schisandrin A in alleviating age-related hearing loss, paving the way for research into its clinical application and the improvement of patient outcomes.

Declarations

Conflict of Interest:

The authors declare no conflict of interest.

Ethical approval

Because no human subjects or animal experiments were directly involved in this study. Therefore, no additional ethical approval was required.

Consent to participate

For the bioinformatics analysis, all datasets used are publicly available and de-identified, so informed consent was not applicable.

Consent to publish

All authors consent to publication. The study did not include identifiable individual data or clinical images requiring specific consent.

Competing interests

The authors declare that the research was conducted in the absence of any commercial or financial relationships that could be construed as a potential conflict of interest.

Author Contribution

[Author 1 Liangliang Wang]: Conceptualization,study design, analysis and interpretation of data, drafting of the manuscript.[Author 2 Jing Sun]: Network pharmacology data collection, target screening, enrichment analysis, molecular docking and molecular dynamics simulation.[Author 3 Lili Yu]: Supervision, Writing-review and editing , final revision.[Author 4 Qianghe Liu]: Statistical analysis, critical revision of the manuscript for important intellectual content.[Author 5 Fangxian Liu]:Resources, Project administration

Acknowledgements

The authors thank Pubchem, Swiss Target Prediction, Super-PRED for providing publicly available data. This work was supported by Project of Guangxi Natural Science Foundation (Project Contract Number: 2026GXNSFHA00640035) and Guangxi Natural Science Foundation Self-Funded Project(Project Contract Number: 2022JJA140034).

Data Availability

The study was performed based on the Pubchem, Swiss Target Prediction and Super-PRED public databases. The datasets generated and/or analyzed during this study are available in the following public repositories: (1)Pubchem(https://pubchem.ncbi.nlm.nih.gov/); (2)Swiss Target Prediction(http://swisstargetprediction.ch/); (3)Super-PRED(https://prediction.charite.de/index.php); SuperPred 3.0 is described in the following peer-reviewed publication: Gallo, K., Goede, A., Preissner, R., & Gohlke, B.-O. (2022). SuperPred 3.0: drug classification and target prediction—a machine learning approach. Nucleic Acids Research, 50(W1), W726–W731. DOI: 10.1093/nar/gkac297; (4)GeneCards(https://www.genecards.org/);(5)OMIM(https://omim.org/);(6)String(https://string-db.org/);(7)UniProt(https://www.uniprot.org/);(8)Protein data bank(http://www.rcsb.org/pdb).

References

1. Yamasoba, T. et al. Current concepts in age-related hearing loss: epidemiology and mechanistic pathways. *Hear. Res.* **303**, 30–38 (2013).
2. Yang, Z. & Cosetti, M. Safety and outcomes of cochlear implantation in the elderly: A review of recent literature. *J. otology*. **11** (1), 1–6 (2016).
3. Chadha, S., Kamenov, K. & Cieza, A. The world report on hearing, 2021. *Bull. World Health Organ.* **99** (4), 242–242A (2021).
4. Fischer, N., Weber, B. & Riechelmann, H. *[Presbycusis—Age Relat. HearingLoss] Laryngo-Rhino-Otologie* **95** : 497–510. (2016).
5. Falah, M. et al. Association of genetic variations in the mitochondrial DNA control region with presbycusis. *Clin. Interv. Aging*. **12**, 459–465 (2017).
6. Wang, J. & Puel, J. L. Presbycusis: An Update on Cochlear Mechanisms and Therapies. *J. Clin. Med.* **9** (1), 218 (2020).
7. Lowthian, J. A. et al. & ASPREE Investigators Slowing the progression of age-related hearing loss: Rationale and study design of the ASPIRIN in HEARING, retinal vessels imaging and neurocognition in older generations (ASPREE-HEARING) trial. Contemporary clinical trials, **46**, 60–66. (2016).
8. Li, P., Qian, T. & Sun, S. Spatial architecture of the cochlear immune microenvironment in noise-induced and age-related sensorineural hearing loss. *Int. Immunopharmacol.* **114**, 109488 (2023).
9. Qiu, K. et al. The emerging roles and therapeutic implications of immunosenescence-mediated inflammaging in age-related hearing loss. *Am. J. stem cells*. **13** (2), 101–109 (2024).
10. Wang, X. et al. Schisandrin A from Schisandra chinensis Attenuates Ferroptosis and NLRP3 Inflammasome-Mediated Pyroptosis in Diabetic Nephropathy through Mitochondrial Damage by AdipoR1 Ubiquitination. Oxidative medicine and cellular longevity, 2022, 5411462. (2022).
11. Wang, P. et al. Schisandrin A Attenuates Diabetic Nephropathy via EGFR/AKT/GSK3β Signaling Pathway Based on Network Pharmacology and Experimental Validation. *Biology* **13** (8), 597 (2024).

12. Xu, X. et al. Schizandrin prevents dexamethasone-induced cognitive deficits. *Neurosci. Bull.* **28** (5), 532–540 (2012).
13. Jia, S., Guan, H., Zhang, S. & Li, Q. Schisandrin A Alleviates Inflammation and Oxidative Stress in Aβ25-35-Induced Alzheimer's Disease in Vitro Model. *Actas Esp. de psiquiatria*. **52** (5), 724–732 (2024).
14. Hopkins, A. L. Network pharmacology: the next paradigm in drug discovery. *Nat. Chem. Biol.* **4** (11), 682–690 (2008).
15. Li, B., Liu, S., Fang, S., Chen, Y. & Wenxiang Hu Progress in Molecular Docking and Molecular Dynamics Simulation. *J. Comp. Chem.* **3** (1), 1–10 (2019).
16. Kanehisa, M., Furumichi, M., Sato, Y., Matsuura, Y. & Ishiguro-Watanabe, M. KEGG: biological systems database as a model of the real world. *Nucleic Acids Res.* **53** (D1), D672–D677. https://doi.org/10.1093/nar/gkae909 (2025).
17. Kanehisa, M. Toward understanding the origin and evolution of cellular organisms. *Protein science: publication Protein Soc.* **28** (11), 1947–1951. https://doi.org/10.1002/pro.3715 (2019).
18. Kanehisa, M. & Goto, S. KEGG: kyoto encyclopedia of genes and genomes. *Nucleic Acids Res.* **28** (1), 27–30. https://doi.org/10.1093/nar/28.1.27 (2000).
19. Abraham, M. J. et al. *GROMACS: High performance molecular simulations through multi-level parallelism from laptops to supercomputers* 19–25 (SoftwareX, 2015). 1–2.
20. Lindorff-Larsen, K. et al. Improved side-chain torsion potentials for the Amber ff99SB protein force field. *Proteins* **78** (8), 1950–1958 (2010).
21. Wang, J., Wolf, R. M., Caldwell, J. W., Kollman, P. A. & Case, D. A. Development and testing of a general amber force field. *J. Comput. Chem.* **25** (9), 1157–1174 (2004).
22. PatelR.McKinnonB. J. Hearing Loss in the Elderly. *Clin. Geriatr. Med.* **34** (2), 163–174. (2018).
23. Juiz, J. M., Fuentes Santamaría, V., Scheper, V. & Lenarz, T. Editorial: Deafness, aging and Alzheimer's disease: Neurobiological links and therapy options. *Front. NeuroSci.* **16**, 1114383 (2023).
24. Rutherford, B. R., Brewster, K., Golub, J. S., Kim, A. H. & Roose, S. P. Sensation and Psychiatry: Linking Age-Related Hearing Loss to Late-Life Depression and Cognitive Decline. *Am. J. Psychiatry*. **175** (3), 215–224 (2018).
25. Seicol, B. J., Lin, S. & Xie, R. Age-Related Hearing Loss Is Accompanied by Chronic Inflammation in the Cochlea and the Cochlear Nucleus. *Front. Aging Neurosci.* **14**, 846804 (2022).
26. Seidman, M. D., Ahmad, N. & Bai, U. Molecular mechanisms of age-related hearing loss. *Ageing Res. Rev.* **1** (3), 331–343 (2002).
27. López-Otín, C., Blasco, M. A., Partridge, L., Serrano, M. & Kroemer, G. Hallmarks of aging: An expanding universe. *Cell* **186** (2), 243–278 (2023).
28. Paplou, V., Schubert, N. M. A. & Pyott, S. J. Age-Related Changes in the Cochlea and Vestibule: Shared Patterns and Processes. *Front. NeuroSci.* **15**, 680856 (2021).

29. Uraguchi, K. et al. Upregulation of a nuclear factor-kappa B-interacting immune gene network in mice cochleae with age-related hearing loss. *PloS one*, **16**(10), e0258977. (2021).
30. Gu, X. et al. Bioinformatics approach reveals the critical role of inflammation-related genes in age-related hearing loss. *Sci. Rep.* **15** (1), 2687 (2025).
31. Guo, X. et al. Schisandrin A Alleviates Spatial Learning and Memory Impairment in Diabetic Rats by Inhibiting Inflammatory Response and Through Modulation of the PI3K/AKT Pathway. *Mol. Neurobiol.* **61** (5), 2514–2529 (2024).
32. Wang, Q., Liu, L., Guan, H., Zhou, Y. & Li, Q. Schizandrin A ameliorates cognitive functions via modulating microglial polarisation in Alzheimer's disease mice. *Pharm. Biol.* **59** (1), 860–867 (2021).
33. Zong, W. et al. The Antioxidant Phytochemical Schisandrin A Promotes Neural Cell Proliferation and Differentiation after Ischemic Brain Injury. *Molecules (Basel Switzerland)*. **26** (24), 7466 (2021).
34. Iqbal Hossain, M. et al. Dual role of Src kinase in governing neuronal survival. *Brain Res.* **1594**, 1–14. https://doi.org/10.1016/j.brainres.2014.10.040 (2015).
35. Harris, K. C., Hu, B., Hangauer, D. & Henderson, D. Prevention of noise-induced hearing loss with Src-PTK inhibitors. *Hear. Res.* **208** (1–2), 14–25 (2005).
36. Bhatta, P. et al. Capsaicin Protects Against Cisplatin Ototoxicity by Changing the STAT3/STAT1 Ratio and Activating Cannabinoid (CB2) Receptors in the Cochlea. *Sci. Rep.* **9** (1), 4131 (2019).
37. Benkafadar, N. et al. An essential signaling cascade for avian auditory hair cell regeneration. *Dev. Cell*. **59** (2), 280–291e5 (2024).
38. Vijayakumar, S. et al. In silico transcriptome screens identify epidermal growth factor receptor inhibitors as therapeutics for noise-induced hearing loss. *Sci. Adv.* **10** (25), eadk2299 (2024).
39. Karney-Grobe, S., Russo, A., Frey, E., Milbrandt, J. & DiAntonio, A. HSP90 is a chaperone for DLK and is required for axon injury signaling. *Proc. Natl. Acad. Sci. U.S.A.* **115** (42), E9899–E9908 (2018).
40. Liu, Q. et al. Hypoxia-Stabilized HIF1α Restricts Hair Cell Reprogramming by Suppressing Wnt Signaling in the Mammalian Cochlea. *Cells* **15** (16), 1440 (2026).
41. Dai, Z. J. et al. Up-regulation of hypoxia inducible factor-1α by cobalt chloride correlates with proliferation and apoptosis in PC-2 cells. *J. experimental Clin. cancer research: CR*. **31** (1), 28 (2012).
42. Yang, H. & Chen, C. Cyclooxygenase-2 in synaptic signaling. *Curr. Pharm. Design*. **14** (14), 1443–1451 (2008).
43. Narumiya, S. Physiology and pathophysiology of prostanoid receptors. Proceedings of the Japan Academy. Series B, Physical and biological sciences, 83(9–10), 296–319. (2007).
44. Zhuang, J. et al. Targeting MicroRNA-125b Promotes Neurite Outgrowth but Represses Cell Apoptosis and Inflammation via Blocking PTGS2 and CDK5 in a FOXQ1-Dependent Way in Alzheimer Disease. *Front. Cell. Neurosci.* **14**, 587747 (2020).
45. Min, L., You, Y., Ren, S. & Chen, C. Multi-Omics Integration Identifies PTGS2 as a Candidate Diagnostic Biomarker and Precise Therapeutic Target Related to Schisandra chinensis for Osteoarthritis. *Chem. Biol. Drug Des.*, **108**(2), e70368. (2026).

Figures

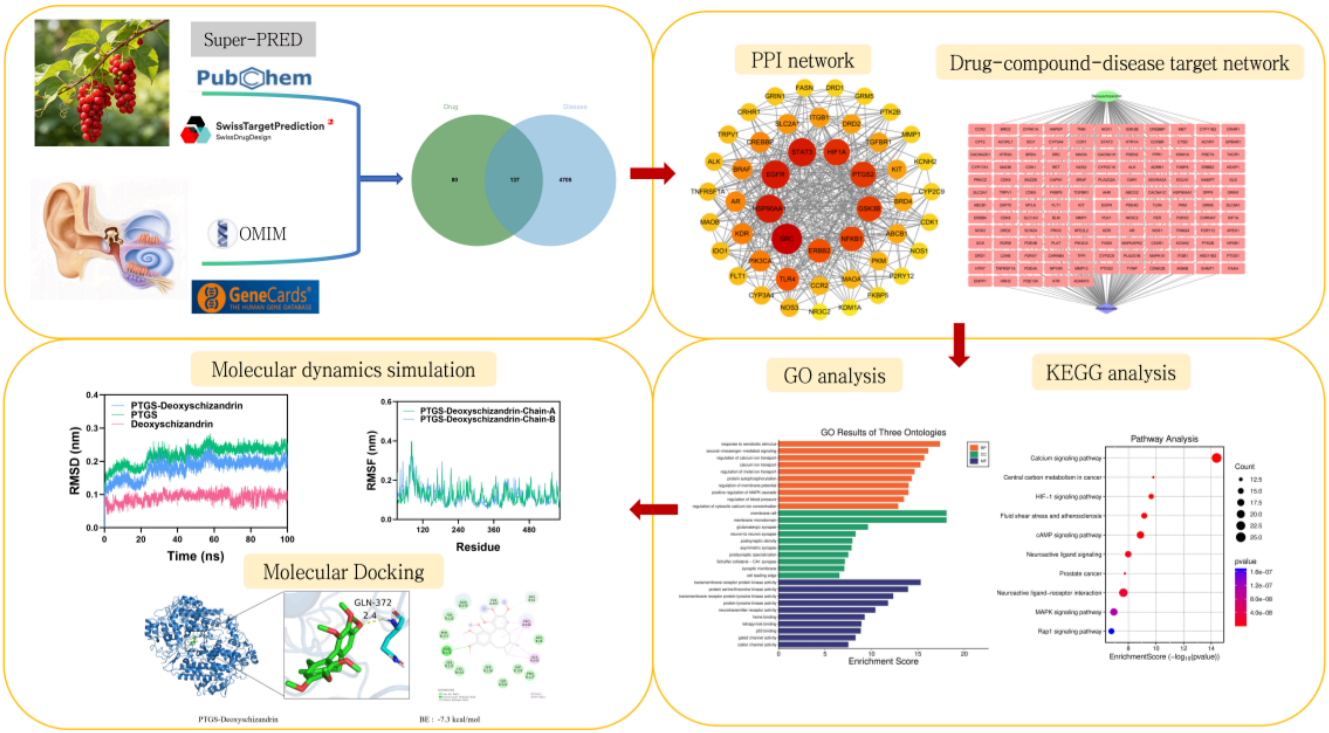


Figure 1. Graphical representation of the workflow of this study

Figure 1

See image above for figure legend

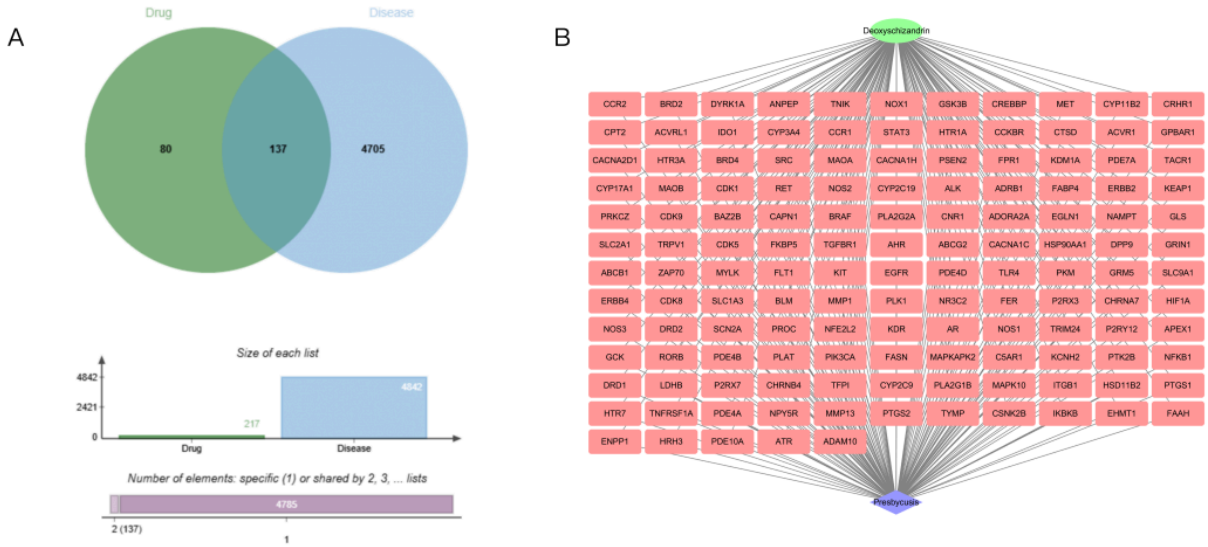


Figure 2. (A) Common targets were identified by taking an intersection of drug-target genes and OS-related genes. The green circle stands for the targets of SchA, The blue circle stands for the targets of ARHL; (B) Network diagram of drug-ingredients-targets

Figure 2

See image above for figure legend

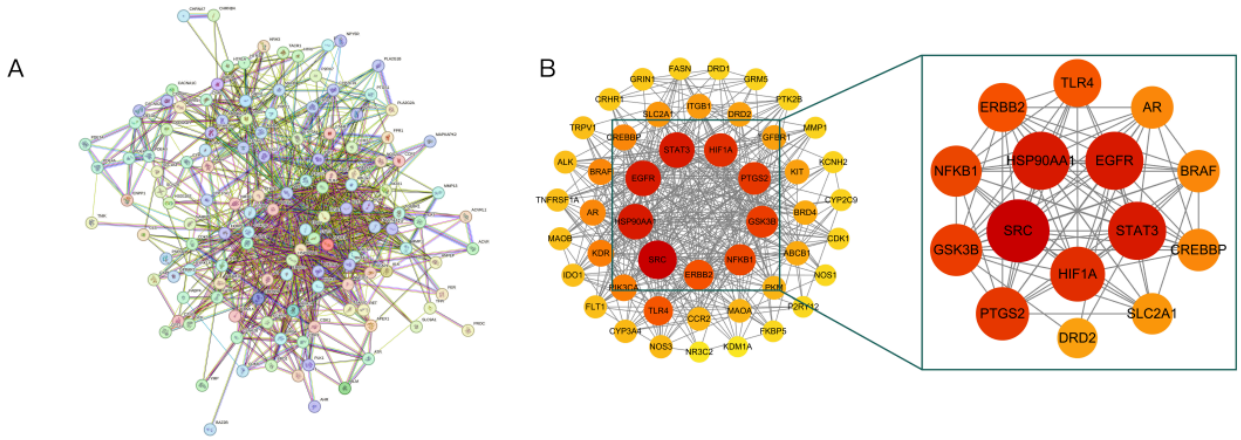


Figure 3. PPI Network Diagram of Potential and Core Targets. (A) the original PPI (protein–protein interaction) network; (B) the core target network after screening.

Figure 3

See image above for figure legend

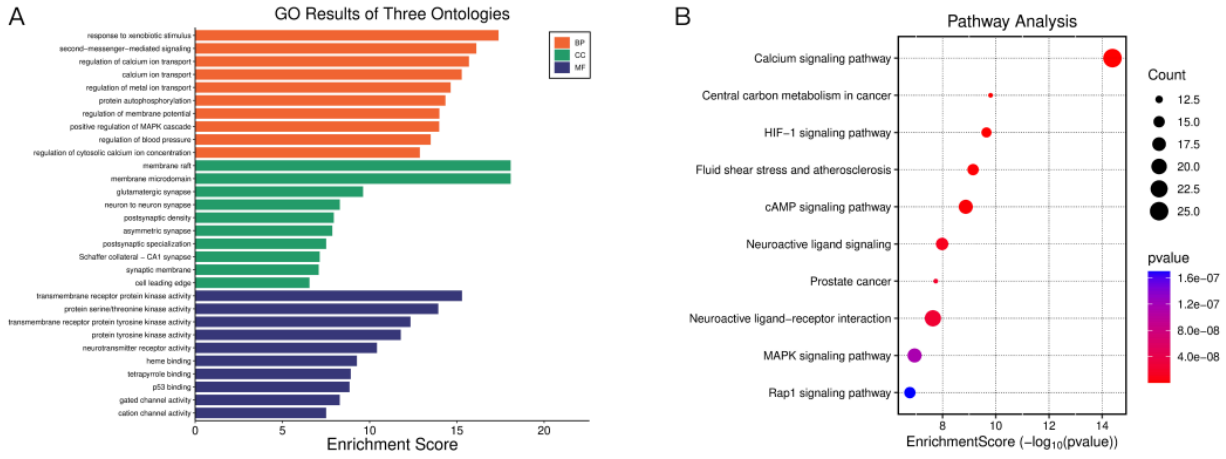


Figure 4.(A) GO (Gene Ontology) biological function analysis results; (B) KEGG pathway enrichment analysis for the targets in SchA treating ARHL;

Figure 4

See image above for figure legend

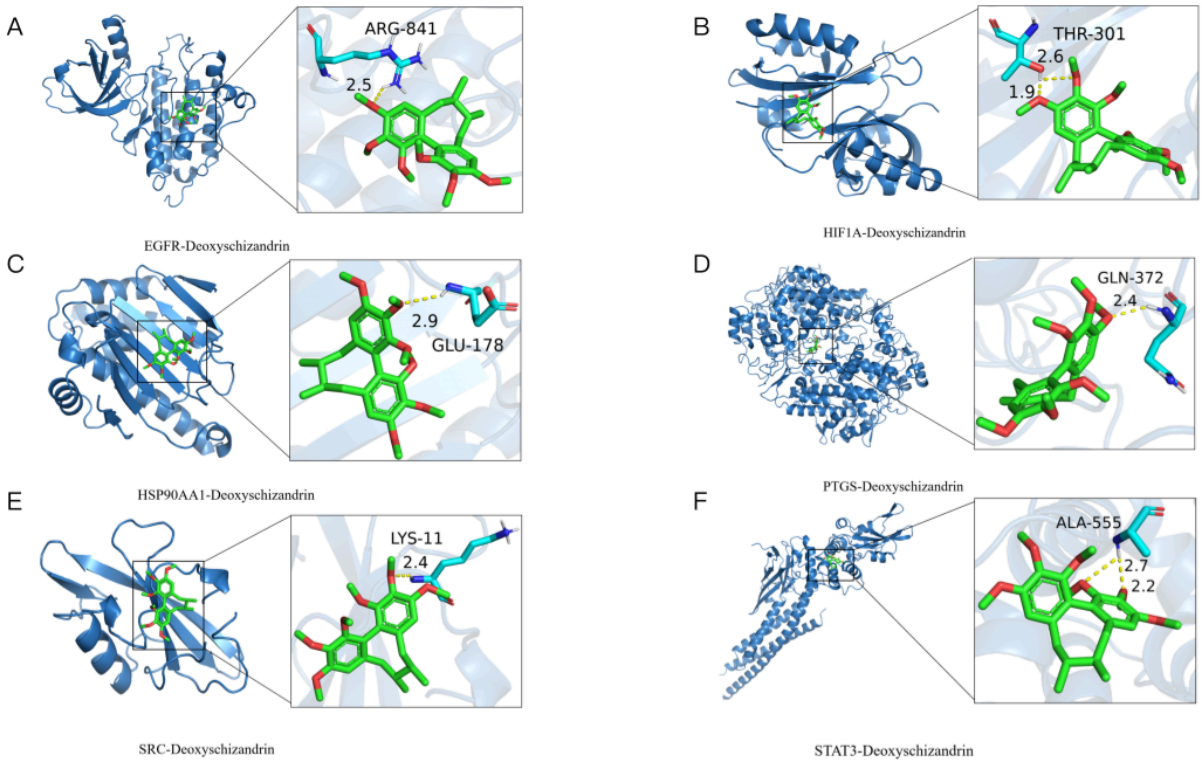


Figure 5. Visualization of the docking and binding of quercetin with three core targets. (A) EGFR-Deoxyschizandrin; (B) HIF1A-Deoxyschizandrin; (C) HSP90AA1-Deoxyschizandrin;(D)PTGS-Deoxyschizandrin;(E)SRC-Deoxyschizandrin;(E)STAT3-Deoxyschizandrin

Figure 5

See image above for figure legend

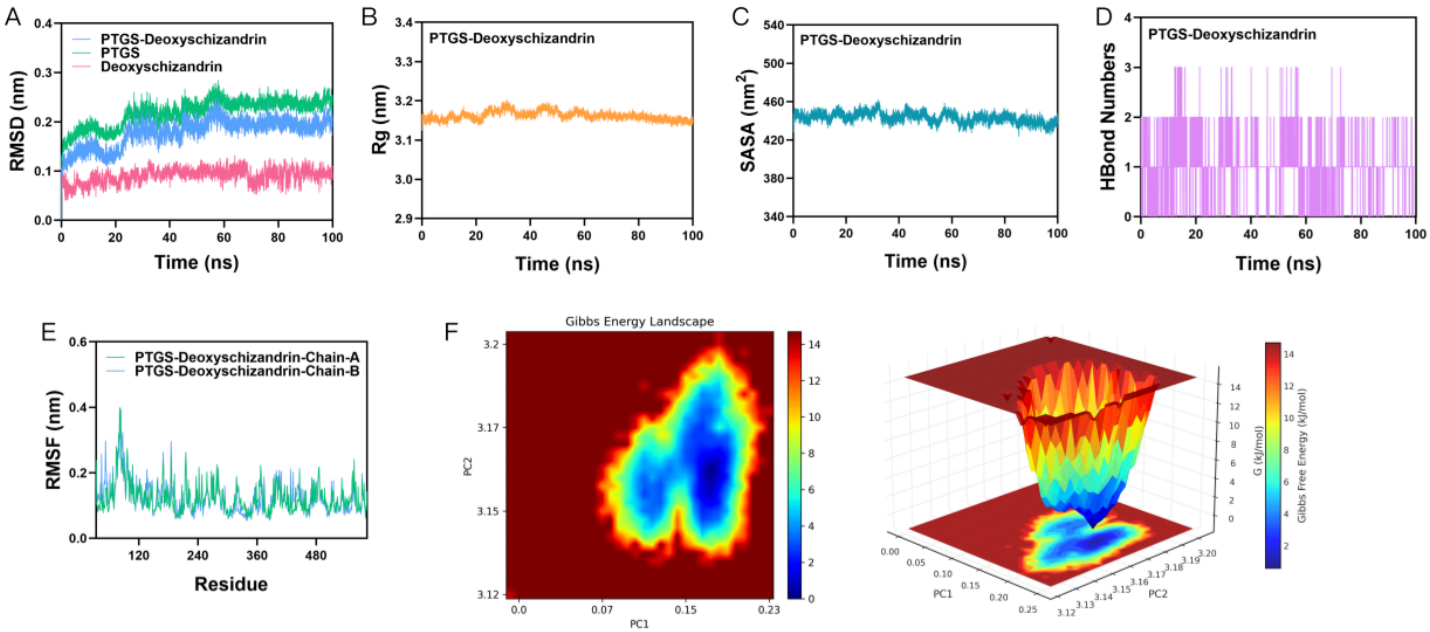


Figure 6. The molecular dynamics simulation trajectories: (A) root mean square deviation of the PTGS-Deoxyschizandrin; (B) radius of gyration of the complex; (C)solvent-accessible surface area of the complex ; (D) hydrogen bonds of the complex; (E)root mean square fluctuation of the complex; (F)Free Energy Landscape

Figure 6

See image above for figure legend